JEE Journal of Ecological Engineering

Journal of Ecological Engineering, 25(12), 83–92
https://doi.org/10.12911/22998993/193752
ISSN 2299–8993, License CC-BY 4.0

Received: 2024.09.24
Accepted: 2024.10.20
Published: 2024.11.01

Influence of Ammonia Concentration on Struvite Production and Ammonia Removal Efficiency in Continuous Flow Crystallizer Reactor

Raudhatul Ulfa[1,2], Izarul Machdar[1,3*], Yunardi Yunardi[1,3], Suhendrayatna[1,3]

[1] School of Engineering, Postgraduate, Universitas Syiah Kuala, Jalan Teungku Syech Abdur Rauf, Darussalam, Banda Aceh 24415, Indonesia

[2] Department of Chemical Engineering, Universitas Malikussaleh, Jalan Batam, Bukit Indah, Lhokseumawe 24355, Indonesia

[3] Department of Chemical Engineering, Faculty of Engineering, Universitas Syiah Kuala, Jalan Teungku Syech Abdur Rauf, Darussalam, Banda Aceh 24415, Indonesia

* Corresponding author's e-mail: machdar@usk.ac.id

ABSTRACT

Ammonia recovery from wastewater is crucial for mitigating environmental impact and complying with regulatory standards. Therefore, this study aimed to explore the potential of a pilot scale continuous flow crystallizer reactor to recover ammonia from urea fertilizer plant wastewater through struvite crystallization. On the basis of the principles validated in previous batch experiments, continuous flow crystallizer reactor was designed and operated using identified optimal parameters. Reactor was fed with synthetic wastewater containing ammonia concentration of 500–1000 mg/L and operated under varying hydraulic retention times of 3–5 hours. The influent concentrations of $MgCl_2 \cdot 6H_2O$ and KH_2PO_4 were adjusted to match the ammonia concentration in reactor, maintaining a molar ratio of $Mg:NH_4:PO_4$ at 1:1:1, with pH between 9 and 10. The results showed that over 90% of ammonia was removed and recovered as struvite crystals, with a mean size of 0.1 to 1 mm, allowing for effective sedimentation and harvesting. This showed that the reactor could potentially handle higher loading and achieve greater removal rates. Furthermore, effluent concentration met the standards set by the Indonesian government for the urea fertilizer sector, specifically for discharge into seawater. The study showed the feasibility of using continuous flow crystallizer reactor for efficient ammonia recovery through struvite crystallization. This method reduced the ammonia levels in the effluent, thereby mitigating environmental impact, and produced struvite, which could be used as a slow-release fertilizer to improve economic value. The promising results suggested the potential for further development and industrial application of this method to address the environmental and economic challenges associated with ammonia-containing wastewater.

Keywords: ammonia wastewater, crystallizer reactor, struvite crystal, urea fertilizer plant.

INTRODUCTION

The annual production of urea fertilizer in Indonesia is estimated to be approximately 9.36 million tons, with an annual usage growth of 1.7%. This amount is supplied by various companies, such as PT Pusri, PT Kujang, PT Kaltim, PT PIM, and Petrokimia Gresik (Indonesia Fertlizer, 2023). In the process of producing urea, 0.3 tons of water is generated for every ton, containing ammonia (2–99 wt%), carbon dioxide (0.8–6 wt%), and urea (0.3–1.5 wt%) (Rahimpour et al., 2010, Laghari et al., 2018). Previous studies have shown that the effluents from urea manufacturing facilities lead to a decrease in water quality, exceeding permissible limits for parameters such as ammonia content, urea concentration, and pH (Sanni et al., 2021, Scherger et al., 2021, Matijašević et al., 2010). In Indonesia, urea fertilizer plants commonly use ammonia stripping towers to reduce

the ammonia levels in wastewater (Machdar et al., 2018). However, the method can face difficulties in complete eradication of ammonia when the levels in the wastewater fluctuate. These difficulties occur from the dependence on wastewater dispersion and air velocity during the elimination process. The emission of ammonia into the air can also lead to unpleasant smells near the plant. Furthermore, the use of the stripping towers is associated with various drawbacks, such as the need to add lime for pH control, high energy consumption and maintenance for pumping, as well as issues with air pollution (EPA, 2000).

Removal or recovery of ammonia nitrogen from wastewater is a crucial aspect of environmental management, which has gained significant attention through various innovative methods. Previous studies have explored different methods, such as using gas-permeable membranes for efficient removal and recovery of ammonia-nitrogen (Yan et al., 2023), negatively charged membranes in direct contact membrane distillation systems for high ammonia recovery rates (Kywe and Ratanatamskul, 2022). Other methods include the application of electrodeionization with supporting electrolytes to enhance threcovery efficiency (Xu et al., 2022), as well as ammonia removal by simultaneous nitrification and denitrification (Kondaveeti et al., 2022). Despite these advancements, there are still difficulties in identifying a suitable technology that effectively recovers ammonia to produce valuable materials, while simultaneously improving the quality of the wastewater effluent.

The majority of previous treatment methods have typically focused only on elimination. Recently, significant advancement was made towards simultaneously removing and recovering ammonia nitrogen in the form of magnesium ammonium phosphate hexahydrate, also known as struvite. According to the results, struvite showed great potential as a slow-released fertilizer, particularly beneficial for crops requiring low-solubility fertilizers. The solubility of struvite in wastewater was found to be 3.89×10^{-10} at 25 °C, while 4.330×10^{-14} at 25 °C in aqueous solution (Bhuiyan et al., 2007). Moreover, struvite does not have a negative impact on plant roots (Priestley et al., 1997, Gaterell et al., 2000).

The production of struvite crystals from different wastewater types has been extensively discussed by Rahman et al., (2013). These crystals form under alkaline conditions, as shown in Equation 1 (Bouropoulos and Koutsoukos, 2000). In an aqueous solution, the formation occurs following the development of supersaturation, which is the driving force behind all crystallization processes (Pastor et al., 2008). This process occurs relatively quickly due to the excess supersaturation in the liquid from the chemical reaction between magnesium, ammonium, and phosphate. The kinetics of struvite crystal formation have been studied by Crutchik and Garrido (2016), who expressed the reaction using a first-order kinetic model.

$$Mg^{2+} + NH_4^+ + H_2PO_4^- + 6H_2O \rightarrow MgNH_4PO_4 \cdot 6H_2O + 2H^+ \quad (1)$$

The operational mode of the crystallization reactor is essential in struvite production. Several efforts have been implemented to achieve high removal rates of ammonia and phosphate by precipitating struvite from wastewater using various reactor types. Le Corre et al. (2007) designed a pilot-scale crystallization reactor with continuous feed of synthetic solution. The reactor was equipped with two concentric stainless steel mesh screens submerged at the top of reactor. It was found that by combining the two meshes, struvite could be accumulated at a rate of 7.6 g/m² per hour under optimal conditions.

Suzuki et al. (2007) developed continuous flow reactor with three layers of stainless steel mesh to provide aeration and sedimentation zones. The results showed that 65 kg of struvite was obtained over 70 days of operation with an influent rate of 5.3 m³ per day. Ali and Schneider (2008) designed a batch reactor equipped with an automatic temperature control and feed system. The reactor had a volume of 44 liters and was made from acrylic sheets. A control system was used to maintain the pH level and adjustment was made when the value was below the set point. Two dosing pumps operated based on the output signal from the pH controller.

Rahman et al. (2011) designed a continuous reactor made of plexiglass with a volume of 12.3 liters. Wastewater influent and $MgCl_2$ solution were fed into the reaction zone where air was introduced at a rate of 0.73 liters per minute. This system produced white crystals of irregular size and achieved removal efficiency of 93% for PO_4 and 31% for ammonia. Hunik et al. (2012) designed a crystallization reactor made from a glass cylinder equipped with a heating and cooling jacket. Reactor included a draft tube and three paddle-type stirrers. PO_4, Mg, and NH_4 were added in ratios of 1:1:1 and 1:1.2:1 under various pH values as well as constant temperatures.

Matynia et al. (2013) reported that struvite crystals were successfully produced in continuous operation using a jet-pump crystallizer. Ha et al. (2023) designed a fluidized-bed reactor for struvite granulation, investigating various hydraulic parameters, such as pH and cross-sectional surface loading. Despite the modifications and improvements in recovery efficiency, there is still a need to explore reactor designs that effectively treat ammonia-containing wastewater, such as the discharge from urea fertilizer industry to generate struvite.

On the basis of the description, this study aimed to design a continuous flow reactor with two sections, namely a reaction zone and a settling zone. Before this study was carried out, batch experiments were conducted to determine the optimal operating parameters for setting up continuous pilot scale system (Machdar et al., 2018). The specific objectives were to evaluate reactor's performance at different ammonia influent concentration and hydraulic retention times using artificial wastewater, representing the effluent from a urea fertilizer industry. The result was expected to generate struvite and lower ammonia concentration in wastewater to comply with the ammonia effluent standards set by Indonesian government for urea fertilizer sector.

MATERIALS AND METHODS

Reactants (feed preparation)

Synthetic wastewater containing struvite constituent ions was used as influent. Meanwhile, the salts used to prepare the influent feed were commercial-grade magnesium chloride hex-anhydrate ($MgCl_2 \cdot 6H_2O$), potassium dihydrogen phosphate (KH_2PO_4), and ammonium chloride (NH_4Cl). Stock solutions were prepared by dissolving these reactants in distilled water. Depending on the desired experimental conditions, different concentration of KH_2PO_4 (0.404 and 3.865 mmol/L), NH_4Cl (2.991–34.585 mmol/L), and $MgCl_2 \cdot 6H_2O$ (0.738–6.738 mmol/L) were prepared and fed to reactor every 1 to 2 days from a 60 liter influent holding tank. Subsequently, a 70% KOH solution was prepared to adjust the pH level.

Experimental set-up and operation

The pilot setup included a crystallization reactor, three peristaltic pumps, and three feed tanks containing stock solutions of $MgCl_2 \cdot 6H_2O$, NH_4Cl, and KH_2PO_4, respectively. The reactor was equipped with a pH meter and a small injection pump for KOH to adjust liquid pH to the desired range of 8–9.

The crystallizer reactor was a cylindrical tank constructed from Plexiglas, with a total capacity of 90 liters. It was divided into two sections, namely the upper part serving as the reaction and crystal growth area, measuring 40 cm in height and diameter. Meanwhile, the lower part served as the settling zone, measuring 40 cm in height and 30 cm in diameter. An internal circulator pushed the reactant downward through a draft tube installed in the upper section to prevent the loss of fine crystal struvite particles in the effluent. Effluents exited the top part through a circular V-notch weir. The reactor used a small axial flow propeller as an agitator to reduce resistance and enhance thrust (Samaras et al., 2006). The agitator was operated at a speed of 100 rpm. Struvite products were collected at the bottom of reactor and were periodically discharged by opening the bottom valve. The schematic diagram and photograph of reactor are shown in Figure 1.

The reactor operation was divided into three distinct experimental periods to determine the impact of influent ammonia concentration on removal percentage and methodology. These periods comprised varying concentration of 500 (day 0–28), 750 (day 29–55), and 1000 mg/L (day 56–86). The influent concentration of $MgCl_2 \cdot 6H_2O$ and KH_2PO_4 were adjusted to match ammonia concentration applied to reactor, maintaining a molar ratio of $Mg:NH_4:PO_4$ as 1:1:1, respectively. The performance of reactor in each experimental period was assessed under HRT of 3, 4, and 5 hours by adjusting the reactant flow rates. Subsequently, effluent samples were collected daily, filtered through a 0.45 mm membrane, and preserved for chemical analysis.

Tracer study

A saturated aqueous solution of sodium chloride (NaCl) was used to examine the hydraulic properties of the crystallizer reactor. The solution was added to the reactor influent using a pulse input. A high concentration of NaCl was selected to minimize the quantity used and avoid any disruption to the incoming flow. A digital conductivity meter was used to continuously measure the NaCl content at the reactor outlet, enabling the calculation of residence time distribution (RTD) curves.

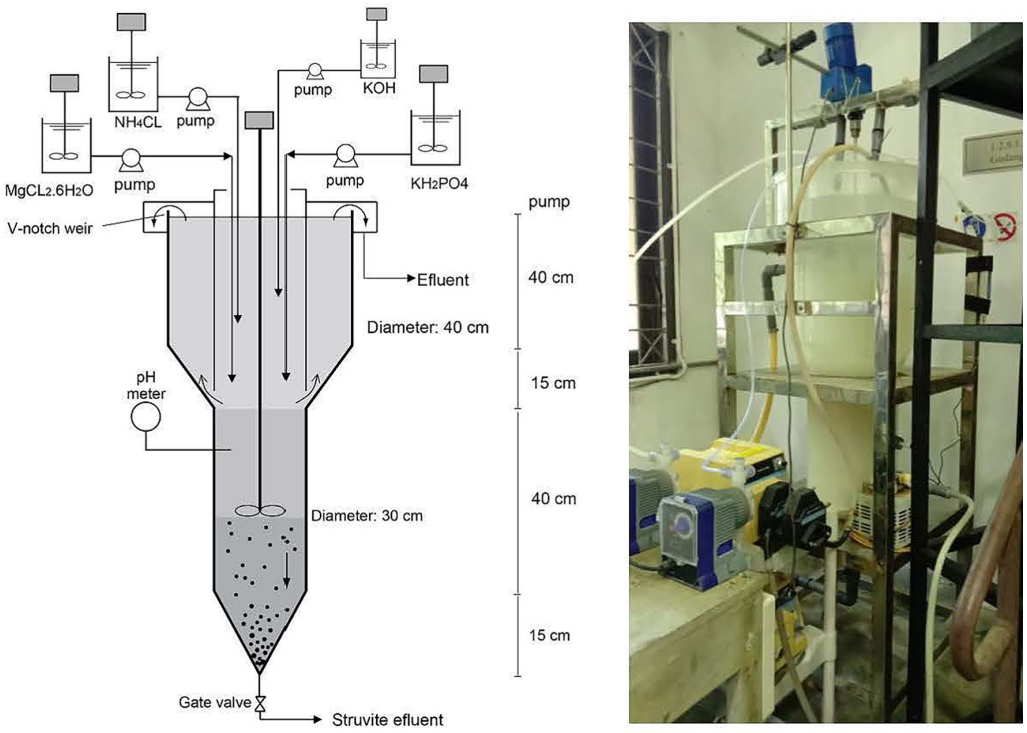

Figure 1. Schematic diagram and photograph of reactor

Replicated experiments were carried out with flow rates ranging from 30 to 50 L/h and varying agitator speeds between 100 and 180 rpm. From RTD curves, Levenspiel (1999) provided the methods used to establish the average actual hydraulic retention time (HRT). Meanwhile, the theoretical HRT was calculated by dividing reactor volume by the flow rate. The active volume percentage of reactor was determined by dividing the theoretical HRT by the actual value.

Analytical methods

The filtered samples were examined for ammonia concentration through a UV-VIS spectrophotometer (Shimadzu UV-1700), followed by adding Nessler reagent and sodium potassium tartrate. SEM-EDS (JEOL JSM 6510) and FTIR (Shimadzu IRPrestige-21) were used to investigate the surface characteristics and chemical bonds in a molecule of struvite crystal.

RESULTS AND DISCUSSIONS

Tracer study

This investigation included conducting duplicate tests for flow rates of 50, 40, and 30 L/h, which corresponded to HRT of 1.8, 2.25, and 3 hours, respectively. Figure 2 shows the representative RTD curve and offers a detailed interpretation of the summarized data. Theoretical HRT represents the ideal duration for fluid to pass through the crystallizer reactor based on design parameters. Meanwhile, the actual HRT shows the observed real-time duration during the operation. By comparing these two values, the active volume percentage provides insight into the extent to which reactor operates based on intended capacity, enabling the detection of deviations or inefficiencies in the system.

Figure 2 facilitates the analysis of how fluid dynamics influence the flow pattern within reactor. The results showed that the actual HRT was generally shorter than the theoretical for each test. This discrepancy could be attributed to the presence of a flow pattern in the form of a short-circuiting (Khaatoon et al., 2023) or a dead volume (Sheoran et al., 2018) within the reactor. The RTD curve showed the short-circuiting phenomenon in the reactor, showed by the rapid increase in concentration of the inert tracer to a maximum peak, along with continuous decrease back to the initial concentration. An in-depth review of short-circuiting in a continuous stirred-tank reactor is provided by Nechita et al., (2023). Analysis of the tracer data showed that the active volume ranged

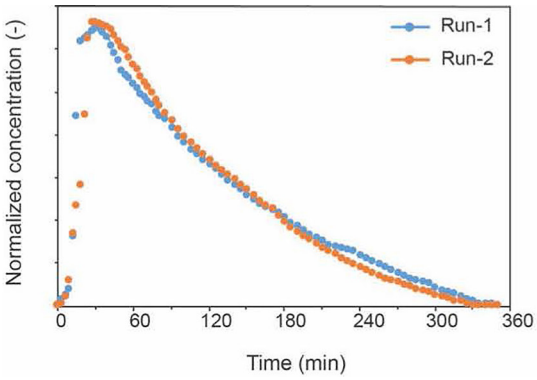

Agitation speed (rpm)	HRT (h)		Active volume (%)
	Theoretical	Actual	
100	3.0	1.92 ± 0.05	63.96 ± 1.71
	2.25	1.94 ± 0.12	85.15 ± 5.31
	1.8	1.59 ± 0.06	88.11 ± 3.60
130	3.0	2.03 ± 0.17	67.72 ± 5.73
	2.25	2.18 ± 0.14	97.10 ± 6.09
	1.8	1.72 ± 0.07	95.75 ± 3.81
180	3.0	2.02 ± 0.08	67.36 ± 2.70
	2.25	1.70 ± 0.14	75.49 ± 6.08
	1.8	1.55 ± 0.02	86.35 ± 0.88

Figure 2. Representative RTD curve and tracer summarized data

from 63.96% to 97.10%. The variation in agitation speed between 100 and 180 rpm had no significant impact on the active volume. However, a decrease in flow rate led to a reduction in the active volume. This phenomenon can be attributed to the diminished turbulence, which caused reduced impeller movement. Visual observations showed that increased turbulence had a negative effect on the sedimentation of struvite crystals, disrupting the settling process. This disruption could lead to decreased efficiency and potential operational concerns within the reactor. Therefore, it is recommended to keep agitation levels at a minimum to promote proper sedimentation and ensure optimal reactor performance. By reducing turbulence, the reactor can achieve a more stable environment, facilitating the efficient separation and collection of struvite crystals.

Effect of ammonia influent concentration and HRT on removal efficiency

The effects of varying ammonia influent concentration and HRT on the effluent concentration are shown in Figure 3. Specifically, Figure 3a shows ammonia effluent concentration when the influent concentration is maintained at 500 mg/L. The average effluent concentration observed at HRT of 3, 4, and 5 hours were 65.2 ± 10.1 mg/L, 57.4 ± 14.4 mg/L, and 54 ± 9.5 mg/L, respectively. These results corresponded to average ammonia removal efficiencies of 87 ± 2%, 89 ± 3%, and 89 ± 2% for HRT of 3, 4, and 5 hours, respectively. The data showed that there was no significant difference in removal performance between the HRT of 3, 4, and 5 hours. Therefore, varying the HRT within this range did not significantly impact the

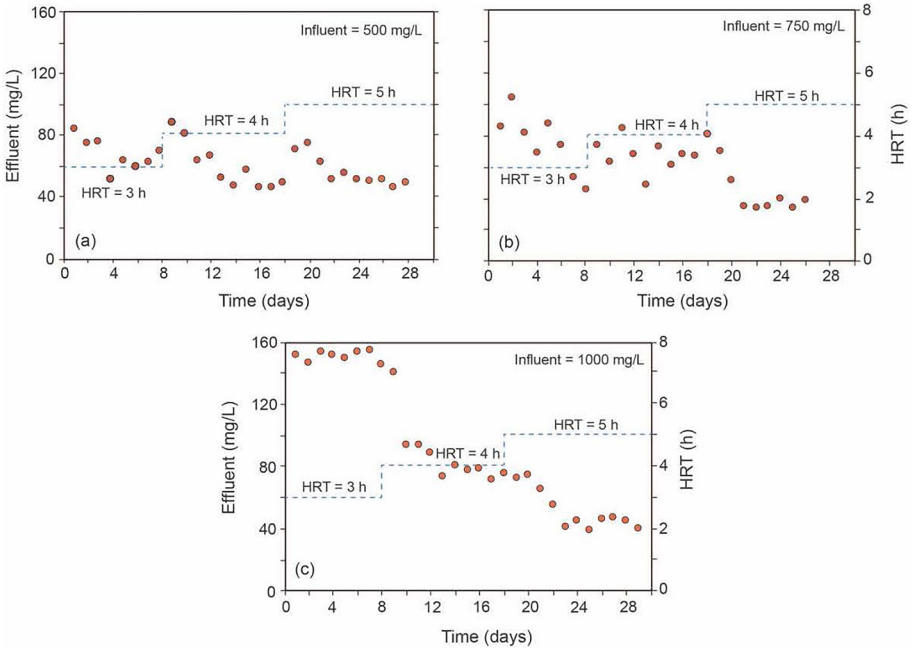

Figure 3. Effects of varying ammonia influent concentration and HRT on the effluent concentration

effluent ammonia concentration or the overall removal efficiency. Figure 3b shows the ammonia levels in the effluent with influent concentration fixed at 750 mg/L. At HRT of 3, 4, and 5 hours, the effluent ammonia concentration was recorded as 75.8 ± 19.1 mg/L, 68.4 ± 9.7 mg/L, and 47.4 ± 17.4 mg/L, respectively. Corresponding removal efficiencies were 90% ± 3%, 91% ± 1%, and 94% ± 2%, for the 3, 4, and 5-hour HRTs. However, no significant differences were observed in removal efficiencies between the 3 and 4-hour periods. The 5-hour period showed a slightly improved average removal efficiency, suggesting a modest improvement in performance with extended retention times, compared to shorter times of 3 and 4 hours.

Figure 3c shows the ammonia concentration in the effluent when the influent concentration is set at 1000 mg/L. At an HRT of 3 hours, the average ammonia effluent concentration was 149.7 ± 4.7 mg/L. When HRT was increased to 4 hours, the average concentration dropped significantly to 80 mg/L, with an SD of 8.3 mg/L. Further increase in the HRT to 5 hours led to 46.6 mg/L, with an SD of 7.9 mg/L. This concentration corresponded to average ammonia removal efficiencies of 85 ± 0.5%, 92 ± 0.8%, and 95 ± 0.8% at, 3, 4, and 5 hours. The data showed that extending the HRT from 3 to 4 hours significantly increased removal efficiency, but no substantial difference was observed at 4 and 5 hours. This showed that operating the system with an influent ammonia concentration of 1000 mg/L had the most significant improvement in removal efficiency when increasing the HRT from 3 to 4 hours. Beyond this point, removal efficiency stabilized, and further extension did not have a significant effect. A comprehensive summary of how varying influent ammonia concentration impacts removal efficiency across different HRT is shown in Figure 4. The data showed the relationship between concentration of ammonia entering the system and removal efficiency at retention times of 3, 4, and 5 hours. For influent concentration of 500 mg/L, the system achieved high efficiency across all tested HRT, with no significant differences between 3, 4, and 5 hours. This showed that at the shortest retention time of 3 hours, the system could maintain high removal efficiency.

As the influent concentration increased from 500 mg/L to 750 mg/L, removal efficiency remained robust but began to show more variation between the different HRTs. At this higher concentration, efficiency at a 3-hour HRT was slightly lower compared to the 4-hour and 5-hour HRT. Efficiency improved significantly at a 4-hour HRT, and further enhancements were observed at 5 hours, although at a lower rate.

For the highest influent concentration tested, 1000 mg/L, the data showed more significant differences in removal efficiency across HRT. Removal efficiency was lower at a 3-hour HRT. Increasing to 4 hours substantially improved efficiency, while 5-hour HRT offered additional gains at a lower rate. Figure 4 also shows that shorter HRT can maintain high removal efficiencies at lower influent concentration. However, longer HRT is beneficial for higher influent concentration to achieve optimal ammonia removal. The relationship between influent concentration and removal efficiency is dependent on HRT. This shows the importance of adjusting retention times in response to varying influent concentration to maintain high treatment performance. Typical ammonia stripping efficiencies range from 65% to 99%, depending on operating conditions (Guštin and Marinšek-Logar, 2011). While potentially comparable in efficiency, struvite crystallization avoids air pollution and odors associated with

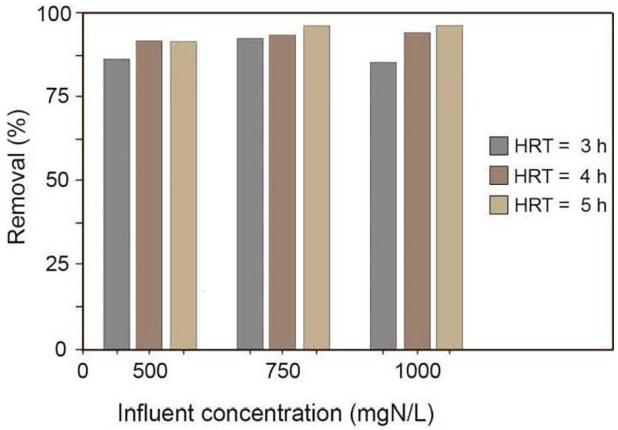

Figure 4. Impact removal efficiency across varying influent ammonia concentration and different HRT

stripping, as noted in the study. Moreover, ammonia stripping poses environmental challenges due to ammonia emissions. Gas-permeable membrane technology, though effective, is associated with higher operational costs. Recent studies on gas-permeable membranes have shown ammonia removal efficiencies of 94–99% (Vanotti and Szogi, 2015). Conventional biological nitrification-denitrification treatments can achieve 60–90% ammonia removal (Metcalf and Eddy, 2014). The struvite crystallization method adopted in this study appears to perform at the higher end of this range.

Loading rate vs removal rate

The quantification ammonia removal rate for struvite production is essential to ensure compliance with effluent limits. On the basis of the results presented in Figure 5, removal rate showed a strong correlation with ammonia loading rate. For all experiments, ammonia removal rate increased with higher influent concentration. The experiments produced linear correlations with R^2 values of 0.99, 0.85, and 0.99 for influent concentration of 500, 750, and 1000 mg/L, respectively, showing a consistent relationship. This consistency suggested that reactor performance remained stable at the higher influent ammonia concentration of 1000 mg/L. The linear relationship between ammonia loading rate and removal rate did not diminish across the tested ranges. This implied that the system could potentially handle higher ammonia loading rates to achieve greater ammonia removal rates.

Struvite crystal product characteristics

A typical example of struvite crystals product from this study including images from SEM-EDS analysis is shown in Figure 6. Struvite product appeared as a white crystalline powders, composed of equimolar concentration of magnesium, ammonium, and phosphate, along with six water molecules. The crystals showed a distinctive orthorhombic structure, as well as cubic and needle-like forms with an average size of 0.1 to 1 mm. Le Corre et al. (2007) also observed similar structures using a pilot crystallization reactor fed with synthetic liquor. Ariyanto et al. (2013) reported similar shapes using a laboratory-scale jacketed stirred batch crystallizer. Additionally, Machdar et al. (2018) using batch experiments observed identical crystalline structures. This consistency across various studies showed the typical morphological characteristics of struvite crystals.

On the basis of the results of EDS examination, the phosphorus peak showed a slight elevation compared to the magnesium peak, as similarly reported by Ariyanto et al. (2014). Struvite is composed of magnesium, ammonium, and phosphate in a balanced molar proportion of 1:1:1. However, variations from this precise stoichiometric ratio may arise during the struvite formation process, leading to unequal concentration of different elements. EDS analysis predominantly captures the surface constitution of the specimen. When the surface of struvite crystals is enriched with phosphorus due to the crystal growth or precipitation mechanisms, it could lead to an increased phosphorus peak.

The analysis of potential alterations in the internal arrangement of struvite crystals was carried out using the FTIR pattern, as shown in Figure 7. The presence of O-H and N-H stretching vibrations was shown by the absorption at 3589 cm^{-1}, indicating the existence of water molecules for hydration (Ariyanto et al., 2013). The absorption occurring

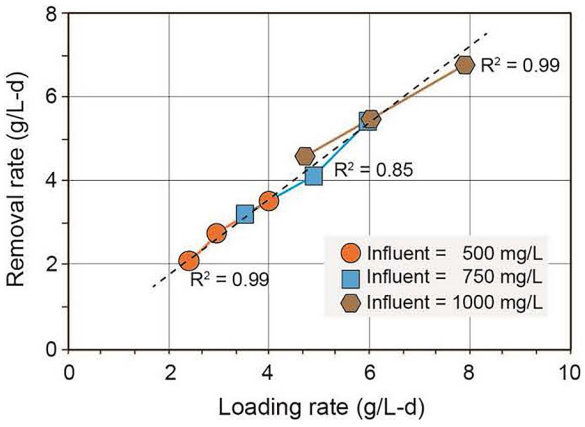

Figure 5. Relation between ammonia loading rate and ammonia removal rate

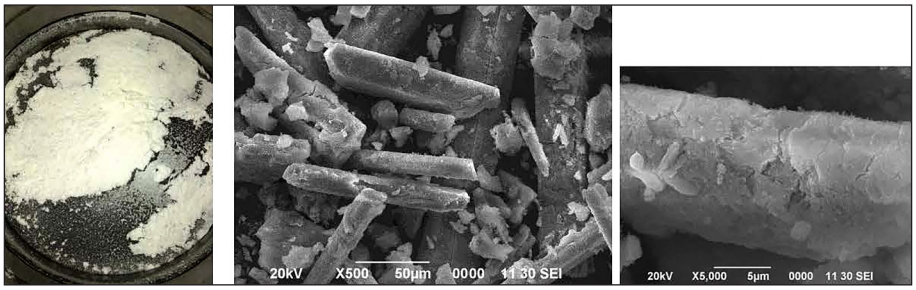

Figure 6. Struvite crystals product and SEM photograph

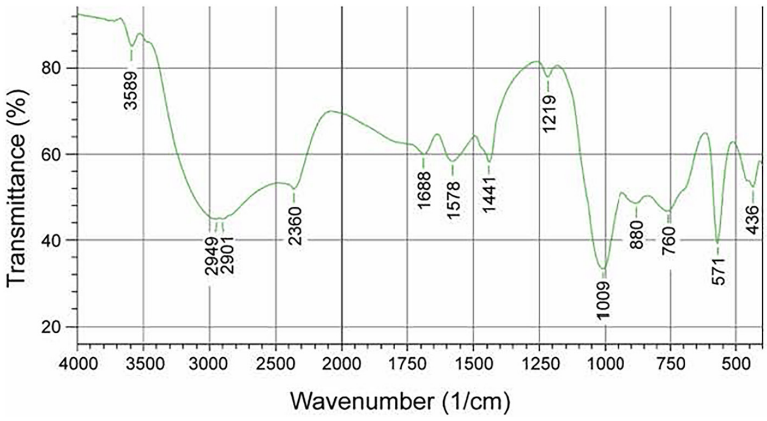

Figure 7. FITR spectrum of struvite crystals

at approximately 2949 cm^{-1} and 2901 cm^{-1} was attributed to the presence of the ammonium ion (Chauhan et al., 2008). The faint band observed at 2360 cm^{-1} in the spectrum was correlated with the stretching vibrations of H-O-H from clusters of water molecules in the crystal. The absorptions at approximately 1688 cm^{-1}, 1578 cm^{-1}, and 1441 cm^{-1} were associated with the bending vibration of N-H (Chauhan et al., 2008, Banks et al., 1975). Meanwhile, the absorption observed at 1009 cm^{-1} could be correlated with the presence of ionic phosphate (Suguna et al., 2012). A moderate absorption at 880 cm^{-1} and 760 cm^{-1} corresponded to the rocking motion of the N-H bond, while the absorption at 571 cm^{-1} could be to the metal-oxygen bond (Chauhan et al., 2008). Therefore, the FTIR spectrum showed the existence of N-H bond, P-O bond, ammonium ion, phosphate ion, water for hydration, and metal-oxygen bond in struvite crystal.

CONCLUSIONS

In conclusion, this study showed the feasibility and effectiveness of using a pilot-scale continuous-flow crystallizer reactor to recover ammonia from urea fertilizer plant wastewater through struvite crystallization. The reactor was continuously operated with parameters optimized from previous batch experiments. Maintaining a molar ratio of $Mg:NH_4:PO_4$ at 1:1:1 and a pH range between 9 and 10 were crucial factors for achieving optimal struvite production. HRT of 3–5 hours facilitated over 90% ammonia removal, showing the efficiency of the reactor. The process achieved high recovery as struvite crystals, with average size of 0.1 to 1 mm, suitable for sedimentation and harvesting. This reduced the ammonia levels in the effluent and provided a valuable by-product for use as a slow-release fertilizer, adding economic value to the treatment process. Ammonia contents in the treated effluent complied with the discharge regulations set by the Indonesian government for urea fertilizer industry, ensuring the sustainability of industrial operations without harming marine ecosystems. The observed linear relationship between ammonia loading and removal rates suggests that the reactor could potentially handle concentrations exceeding 1000 mg/L. However, further studies at concentrations above 1000 mg/L are recommended to confirm performance stability. The successful operation of reactor showed the potential for scaling up to handle higher ammonia loads. Continuous operation mode showed the tendency for industrial applications

requiring consistent performance. Implementing struvite crystallization offered environmental protection and economic gains. Reducing ammonia in effluents mitigated negative effects on aquatic ecosystems, while struvite recovery provided a valuable agricultural resource to promote a circular economy in wastewater management.

Acknowledgement

The authors express their gratitude to the Universitas Syiah Kuala (No. 332/UN11/ SPK/ PNBP/2021), The Ministry of Education, Culture, Research, and Technology of Republic Indonesia (No. 97/UN11.2/PP/SP3/2019-2020), and PT Pupuk Iskandar Muda (PIM) for their support in conducting this research and for providing the resources to enhance the quality of this study.

REFERENCES

1. Ali M.I., Schneider P.A. 2008. An approach of estimating struvite growth kinetic incorporating thermodynamic and solution chemistry, kinetic and process description. Chem. Eng. Sci., 63(13), 3514–3525. doi: 10.1016/j.ces.2008.04.023
2. Ariyanto E. 2013. Crystallisation and dissolution studies of struvite in aqueous solutions, Thesis for Doctor of Philosophy. Curtin University.
3. Ariyanto E., Sen T.K., Ang H.M. 2014. The influence of various physico-chemical process parameters on kinetics and growth mechanism of struvite crystallisation. Adv. Powder Technol., 25(2), 682–694. doi: 10.1016/j.apt.2013.10.014
4. Banks E., Chianelli R., Korenstein R. 1975. Crystal chemistry of struvite analogs of the type MgMPO4.6H2O (M+ = potassium(1+), rubidium(1+), cesium (1+), thallium(1+), ammonium(1+). Inorganic Chemistry. 14(7), 1634–1639. doi: 10.1021/ic50149a041
5. Bhuiyan M.I.H., Mavinic D.S., Beckie R.D. 2007. A solubility and thermodynamic study of struvite. Environ. Technol., 28(9), 1015–1026. doi: 10.1080/09593332808618857
6. Bouropoulos N.C., Koutsoukos P.G. 2000. Spontaneous precipitation of struvite from aqueous solutions. J. Cryst. Growth., 213(3–4), 381–388. doi: 10.1016/S0022-0248(00)00351-1
7. Chauhan C.K., Vyas P.M., Joshi M.J. 2008. Growth and characterization of struvite crystals. Cryst. Res. Technol., 46, 507–512. doi: 10.1002/crat.201000587.
8. Crutchik D, Garrido J.M. 2016 Kinetics of the reversible reaction of struvite crystallisation. Chemosphere. 154, 567–572. doi: 10.1016/j.chemosphere.2016.03.134
9. EPA. 2000. Wastewater technology fact sheet – Ammonia stripping (EPA 832-F-00-019). United States Environmental Protection Agency. 1–7.
10. Gaterell, M.R., Gay, R., Wilson, R., Gochin, R.J., Lester, J.N. 2000. An economic and environmental evaluation of the opportunities for substituting phosphorus recovered from wastewater treatment works in existing UK fertilizer markets. Environ. Technol., 21, 1067–1084. doi: 10.1080/09593332108618050
11. Guštin, S., Logar, R.M. 2011. Effect of pH, temperature and air flow rate on the continuous ammonia stripping of the anaerobic digestion effluent. Process Saf. Environ. Prot., 89, 1, 61–66. doi: 10.1016/j.psep.2010.11.001
12. Ha T.H., Mahasti N.N., Lin C.S., Liu M., Huang Y.H. 2023. Enhanced struvite ($MgNH_4PO_4 \cdot 6H_2O$) granulation and separation from synthetic wastewater using fluidized-bed crystallization (FBC) technology. J. Water Proc. Eng., 53, 103855–103855. doi: 10.1016/j.jwpe.2023.103855
13. Hutnik N., Piotrowski K., Wierzbowska B., Matynia, A. 2012. Continuous reaction crystallization of struvite from water solutions of phosphates(V) in presence of iron(II) ions. J. Environ. Sci. Eng., A., 1, 35–42.
14. Indonesia Fertilizer (in Bahasa). 2023. https://www.pupuk-indonesia.com/. Access: June 17, 2024.
15. Khatoon B., Kamil S., Babu H., Alam M.S. 2023. Experimental analysis of cascade CSTRs with step and pulse inputs. Mater. Today Proc., 78, 40–47. doi: 10.1016/j.matpr.2022.11.037
16. Kondaveeti S., Choi D.H., Noori Md.T., and Min B. 2022. ammonia removal by simultaneous nitrification and denitrification in a single dual-chamber microbial electrolysis cell. Energies, 15, 9171. doi: 10.3390/en15239171
17. Kywe P.P., Ratanatamskul C. 2022. Influences of permeate solution and feed ph on enhancement of ammonia recovery from wastewater by negatively charged PTFE membranes in direct contact membrane distillation operation. ACS Omega, 7(31), 27722–27733. doi: 10.1021/acsomega.2c03673
18. Laghari A.N., Siyal Z.A., Soomro M.A., Bangwar D.K., Khokhar A.J., Soni H.L. 2018. Quality analysis of urea plant wastewater and its impact on surface water bodies. Eng. Technol. Appl. Sci. Res., 8(2), 2699–2703. doi: 10.48084/etasr.1767
19. Le Corre K.S., Valsami-Jones E, Hobbs P., Jefferson B., Parsons S.A. 2007. Struvite crystallisation and recovery using a stainless steel structure as a seed material. Water Res., 41(11), 2449–2456. doi: 10.1016/j.watres.2007.03.002
20. Levenspiel O. 1999. Chemical Reaction Engineering,

3rd ed. New York, USA: John Wiley and Sons.

21. Machdar I., Depari S.D., Ulfa R., Muhammad S., Hisbullah A.B., Safrul W. 2018. Ammonium nitrogen removal from urea fertilizer plant wastewater via struvite crystal production. IOP Conf. Series: Mat. Sci. and Eng., 358(1). doi: 10.1088/1757-899X/358/1/012026
22. Metcalf & Eddy, Inc. 2014. Wastewater Engineering: Treatment and Resource Recovery. 5th Edition. McGraw-Hill InternationL Edition, New York.
23. Matijašević L., Dejanović I., Lisac H. 2010. Treatment of wastewater generated by urea production. Resour. Conserv. Recycl., 54(3), 149–154. doi: 10.1016/j.resconrec.2009.07.007
24. Matynia A., Wierzbowska B., Hutnik N., Mazienczuk A., Kozik A., Piotrowski K. 2013. Separation of struvite from mineral fertilizer industry wastewater. Procedia Environ. Sci., 18, 766–775. doi: 10.1016/j.proenv.2013.04.103
25. Nechita M.T., Suditu G.D., Puițel A.C., Drăgoi E.N. 2023. Residence time distribution: literature survey, functions, mathematical modeling, and case study—diagnosis for a photochemical reactor. Processes, 11(12). doi: 10.3390/pr11123420
26. Pastor L., Mangin D., Barat R., Seco A. 2008. A pilot-scale study of struvite precipitation in a stirred tank reactor: Conditions influencing the process. Bioresour. Technol., 99(14), 6285–6291. doi: 10.1016/j.biortech.2007.12.003
27. Priestley A.J., Cooney E., Booker N.A., Fraser I.H. 1997. Nutrients in wastewaters-ecological problem or commercial opportunity. Proceedings of the 17th Federal Convention of the Australian Water and Wastewater Association, Melbourne, 1, 340–346.
28. Rahimpour M.R., Mottaghi H.R., Barmaki M.M. 2010. Enhancement of urea, ammonia and carbon dioxide removal from industrial wastewater using a cascade of hydrolyser-desorber loops. Chem. Eng. J., 160(2), 594–606. doi: 10.1016/j.cej.2010.03.081
29. Rahman M., Hashem M., Rahman M, Rahman S.M.E., Hossain M.M., Azad M.A.K., Haque M.E. 2013. Comparison of struvite compost with other fertilizers on maize fodder production. J. Environ. Sci. Nat. Resour., 6(2), 227–231. doi: 10.3329/jesnr.v6i2.22123
30. Rahman M.M., Liu Y.H., Kwag J.H., Ra C.S. 2011. Recovery of struvite from animal wastewater and its nutrient leaching loss in soil. J. Hazard. Mater., 186(2–3), 2026–2030. doi: 10.1016/j.jhazmat.2010.12.103
31. Samaras K., Mavros P., Zamboulis D. 2006. Effect of continuous feed stream and agitator type on CFSTR mixing state. Ind. Eng. Chem. Res., 45(13), 4805–4815. doi: 10.1021/ie0600691
32. Sanni S.E., Odigure J.O., Agboola O., Emetere M.E., Okoro E.E., Audu C. 2021. Empirical assessment of ammonia and urea concentrations in wastewater from a pharmaceutical plant: a case study. IOP Conf. Series: Earth and Env. Sci., 665(1), 0–10. doi: 10.1088/1755-1315/665/1/012003
33. Scherger L.E., Zanello V., Lexow C. 2021. Impact of urea and ammoniacal nitrogen wastewaters on soil: Field study in a fertilizer industry (Bahía Blanca, Argentina). Bull. Environ. Contam. Toxicol., 107(3), 565–573. doi: 10.1007/s00128-021-03280-x
34. Sheoran, M., Chandra, A., Bhunia, H., Bajpai, P.K., Pant, H.J. 2018. Residence time distribution studies using radiotracers in chemical industry—A review. Chem. Eng. Comm., 205(6), 739–758. doi: 10.1080/00986445.2017.1410478
35. Suguna K., Thenmozhi M., Sekar C. 2012. Growth, spectral, structural and mechanical properties of struvite crystal grown in presence of sodium fluoride. Bull. Mater. Sci., 35(4), 701–706. doi: 10.1007/s12034-012-0322-6
36. Suzuki K., Tanaka Y., Kuroda K., Hanajima D., Fukumoto Y., Yasuda T., Waki M. 2007. Removal and recovery of phosphorous from swine wastewater by demonstration crystallization reactor and struvite accumulation device. Bioresour. Technol., 98(8), 1573–1578. doi: 10.1016/j.biortech.2006.06.008
37. Vanotti, M.B., Szogi, A.A. 2015. Systems and methods for reducing ammonia emissions from liquid effluents and for recovering the ammonia. U.S. Patent No. 9, 708, 200. Washington, DC: U.S. Patent and Trademark Office. https://patents.google.com / patent/US9708200B2/en
38. Xu L., Liu D., Liu W., Yang J., Huang J., Wang X., He Q. 2022. Ammonia recovery from wastewater as a fuel: effects of supporting electrolyte on ammonium permeation through a cation-exchange membrane. ACS Omega, 7(24), 20634–20643. doi: 10.1021/acsomega.2c00700
39. Yan X., He L., Zhang W., Chen W., Wu J., Yang N., Cai X., Li L., Yan L., Rao P. 2023. Efficient ammonia-nitrogen removal and recovery from wastewater via the continuous flat-sheet gas-permeable membranes reactor pretreatment. J. Water Proc. Eng., 52, 103571–103571. doi: 10.1016/j.jwpe.2023.103571